HHS Public Access

Author manuscript

Oral Oncol. Author manuscript; available in PMC 2024 July 01.

Published in final edited form as:

Oral Oncol. 2023 July ; 142: 106437. doi:10.1016/j.oraloncology.2023.106437.

Therapeutic inhibition of Bmi-1 ablates chemoresistant cancer stem cells in Adenoid Cystic Carcinoma

Sosuke Sahara[1,2], **Kristy A. Warner**[1], **Alexandra E. Herzog**[1], **Zhaocheng Zhang**[1], **Jacques E. Nör**[1,3,4,5]

[1]Department of Cariology, Restorative Sciences, and Endodontics, University of Michigan School of Dentistry, Ann Arbor, Michigan, USA

[2]Department of Otorhinolaryngology/Head and Neck Surgery, Hamamatsu University School of Medicine, Hamamatsu, Japan

[3]Department of Otolaryngology-Head & Neck Surgery, University of Michigan School of Medicine, Ann Arbor, Michigan, USA

[4]Department of Biomedical Engineering, University of Michigan College of Engineering, Ann Arbor, Michigan, USA

[5]University of Michigan Rogel Cancer Center, Ann Arbor, Michigan, USA

Abstract

Objectives: Adenoid Cystic Carcinomas (ACC) typically show modest response to cytotoxic therapy. Cancer stem cells (CSC) have been implicated in chemoresistance and tumor relapse. However, their role in ACC remains unknown. The purpose of this work was to evaluate the impact of targeting ACC CSCs with Bmi-1 inhibitors on resistance to cytotoxic therapy and tumor relapse.

Materials and methods: Therapeutic efficacy of a small molecule inhibitor of Bmi-1 (PTC596; Unesbulin) and/or Cisplatin on ACC stemness was evaluated in immunodeficient mice harboring PDX ACC tumors (UM-PDX-HACC-5) and in human ACC cell-lines (UM-HACC-2A,-14) or low passage primary human ACC cells (UM-HACC-6). The effect of therapy on stemness was examined by salisphere assays, flow cytometry for ALDH activity and CD44 expression, and Western blots for Bmi-1 (self-renewal marker) and Oct4 (embryonic stem cell marker) expression.

Results: Platinum-based agents (Cisplatin, Carboplatin) induced Bmi-1 and Oct4 expression, increased salisphere formation and the CSC fraction *in vitro* and *in vivo.* In contrast, PTC596 inhibited expression of Bmi-1, Oct4 and pro-survival proteins Mcl-1 and Claspin; decreased the number of salispheres, and the fraction of ACC CSCs *in vitro*. Silencing Claspin decreased salisphere formation and CSC fraction. Both, single agent PTC596 and PTC596/Cisplatin

Corresponding Author Jacques E. Nör DDS, PhD, Professor of Dentistry and Otolaryngology, University of Michigan, 1011 N. University Rm. 2500, Ann Arbor, MI, 48109-1078, United States, jenor@umich.edu.

Authors' Contributions

S. Sahara and J.E. Nör contributed to conception, design, data acquisition and interpretation, drafted and critically revised the manuscript. K.A. Warner, A.E. Herzog, Z. Zhang contributed to data acquisition and interpretation, and critically revised the manuscript. All authors gave the final approval and agreed to be accountable for all aspects of the work.

Conflict of interest statement: The authors declare no conflict of interest with this work

combination decreased the CSC fraction in PDX ACC tumors. Notably, short-term combination therapy (2 weeks) with PTC596/Cisplatin prevented tumor relapse for 150 days in a preclinical trial in mice.

Conclusion: Therapeutic inhibition of Bmi-1 ablates chemoresistant CSCs and prevents ACC tumor relapse. Collectively, these results suggest that ACC patients might benefit from Bmi-1-targeted therapies.

Graphical Abstract

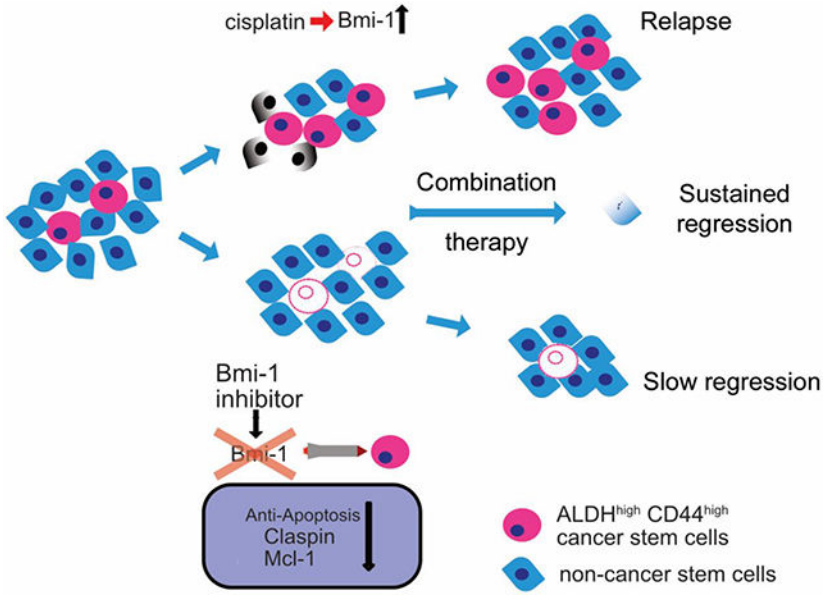

Model of CSC therapy targeting Bmi-1. Platinum-based cytotoxic drugs (*e.g.* Cisplatin) induce Bmi-1 expression, increase ACC stemness, which may lead to tumor relapse. Therapeutic inhibition of Bmi-1 ablates CSCs and suppresses pro-survival genes such as Mcl-1 and Claspin. However, Bmi-1 inhibition is not sufficient to shrink tumors since CSCs constitute a small fraction of tumor cells (<5%). Combination therapy with a cytotoxic drug + Bmi-1 inhibitor may sensitize CSCs to therapy, “debulk” non-CSC tumor cells and cause sustained regression of ACC tumors.

Keywords

Tumor-initiating cell; Self-renewal; Recurrence; Resistance; PTC596; Unesbulin; Salivary gland cancer; Chemotherapy; Head and neck cancer; Claspin

Introduction

Adenoid cystic carcinoma (ACC) is a relentless malignancy that represents approximately 10% of salivary gland tumors [1]. The 5-year and 10-year survival rate of patients with ACC is about 60% and 50%, respectively. However, the 20-year survival rate is only 20%, due to high incidence of tumor relapse and metastases [2]. Lungs constitute the most common site for metastasis, and perineural invasion is characteristic of local progression for ACC [3-5]. The standard treatment for ACC remains surgery with or without radiation

therapy, as there is no systemic therapy with demonstrable safety and efficacy [6]. Although radiation therapy has a positive effect for local disease control, its effect on prolonging overall survival is modest [7,8]. Interestingly, about 30% of patients with distant metastasis do not experience recurrence of the primary lesion [7,9]. Considering the high frequency of disseminated disease, improvements in the long-term survival of ACC patients will require the development of effective systemic therapies.

Cancer Stem Cells (CSCs) constitute a small fraction (≤5%) of the entire tumor cell population. These cells are highly tumorigenic, capable of self-renewal, and capable of regenerating the various cell phenotypes that make up a tumor [10]. These cells are resistant to conventional chemotherapy and have been associated with tumor recurrence and metastasis [11,12]. $ALDH^{high}$ cells generated more tumors than $ALDH^{low}$ cells when transplanted into immunodeficient mice, providing initial evidence for ALDH as a marker for ACC CSC [13]. Further, the Jimeno laboratory showed that $ALDH^{high}CD44^{high}$ cells were more tumorigenic than $ALDH^{low}CD44^{low}$ cells using PDX models of ACC [14]. Considering that CSCs represent a small fraction of overall tumor cells, effective elimination of only CSCs might be insufficient to cause immediate tumor regression. Thus, treatments targeting CSCs are typically accompanied by strategies aiming to eliminate the bulk tumor cells (*e.g.* cytotoxic therapies) [12]. Importantly, effective CSC-targeted therapies have the potential to prevent tumor relapse, as it ablates cells with high tumor-initiating capacity.

Combination therapies involving surgery, radiation and cytotoxic agents (*e.g.* platinum-based agents, 5-FU, paclitaxel) have been frequently used as first line therapy for patients with ACC, despite modest benefits observed with conventional chemotherapy [15]. More recently, targeted agents such as PD-1 inhibitors and anti-angiogenic therapies are being tested particularly in the recurrent/metastatic setting. We and others have shown that platinum-based chemotherapy cause a shift towards self-renewal in tumorigenic CSC in some tumor types, including ACC and head and neck squamous cell carcinoma (HNSCC) [16-18]. Cisplatin increases CSC fraction in HNSCC and induces expression of Bmi-1 (B-cell specific Moloney murine leukemia virus integration site-1), a master regulator of stem cell self-renewal [17]. We showed that CSC-targeted therapies (*e.g.* inhibition of m-TOR pathway, or inhibition of IL-6R) decreases the CSC fraction and is associated with downregulated expression of Bmi-1 in tumors *in vivo* [19,20]. Further, emerging evidence suggest that Bmi-1-positive cells mediate chemoresistance and metastasis in HNSCC [21,22]. A study from the Zhou laboratory showed a significant association between high expression of Bmi-1 and poor ACC metastasis-free survival [23]. The authors concluded that Bmi-1 plays an important role in ACC progression and that Bmi-1 expression can potentially be useful to predict survival. Collectively, these studies indicate that direct inhibition of Bmi-1 might be an attractive target to prevent ACC tumor relapse.

Bmi-1 inhibitors have attracted attention as potential therapeutic agents for cancer. Indeed, small molecule inhibitors of Bmi-1 such as PTC596 (Unesbulin) have shown acceptable safety profiles in phase 1 trials [24]. As such, there are ongoing clinical trials testing PTC596 for cancer treatment (*e.g.* NCT03605550, NCT03761095, NCT03206645). Considering our recent laboratory observations and considering the acceptable safety profile of novel Bmi-1 inhibitors, we decided to evaluate the impact of therapeutic inhibition of

Bmi-1 in preclinical models of salivary ACC [25]. Here, we hypothesized that therapeutic inhibition of Bmi-1 signaling sensitizes ACC CSCs to cytotoxic therapy and prevents tumor relapse.

Material and Methods

ACC patient-derived xenograft (PDX) model

The ACC PDX model used here (UM-HACC-PDX-5) was generated from a primary ACC tumor in the hard palate of a 45-year-old female patient [26]. The specimen that was used to generate the PDX model was collected after maxillectomy without previous radiation or chemotherapy. Histologically, the specimen exhibited cribriform histology and the stage at the time of PDX establishment was considered to be T4aN0M0 (IVa). For these studies, we transplanted fragments of the UM-HACC-PDX-5 tumor (*in vivo* passage 4 to 5) in the subcutaneous space of the dorsal region of female severe combined immunodeficient mice (SCID, CB-17; Charles River; Wilmington, MA, USA), as we showed [27]. Tumor volume was measured using the formula: volume (mm^3) = L x $W^2/2$ (L, length; W, width). Mice transplanted with UM-PDX-HACC-5 tumors were randomly allocated into two groups (n = 6) with an average of tumor volume 300 mm^3. Experimental conditions involved weekly intraperitoneal (i.p.) injections of vehicle (saline) or 5 mg/kg Cisplatin. After 12 days, mice were euthanized, PDX tumors were retrieved and divided into 3 pieces, *i.e.* one for flow cytometry and two smaller pieces for western blots and histology. To evaluate the effect of PTC596 (Selleckchem; Houston, TX, USA) on CSC fraction, tumors were randomly allocated into four groups (n=10). The conditions were as follows; vehicle control; 5 mg/kg Cisplatin; 5 mg/kg PTC596; or combination 5 mg/kg Cisplatin + 5 mg/kg PTC596 regimen. Mice were treated twice (every other day) and euthanized on day 5. For the tumor growth study, mice were randomly allocated to the 4 groups described above and were treated with vehicle, Cisplatin (weekly) and PTC596 (twice a week) for 24 days. To evaluate tumor regrowth after treatment, tumors were randomly allocated as follows: vehicle (n=7), 5 mg/kg Cisplatin, weekly (n =7), or 5 mg/kg Cisplatin (weekly) + 5 mg /kg PTC596 (twice a week) (n= 6). Mice were treated for 2 weeks, then treatment was discontinued and tumors were measured twice/week for 150 days. All *in vivo* experiments followed the ARRIVE (Animal Research: Reporting In Vivo Experiments) guidelines, and an animal protocol (PRO00009324) was reviewed and approved by the Institutional Animal Care and Use Committee (IACUC) of University of Michigan.

Remaining methods can be found in Supplementary Materials.

Results

Platinum-based agents enhance self-renewal and CSC fraction in ACC cells

To investigate the effect of Cisplatin on the fraction of ACC CSCs *in vivo*, we generated PDX ACC tumors and performed a short-term preclinical trial treating mice with 5 mg/kg Cisplatin every 5 days [17]. We allowed tumors to grow to an average 300 mm^3 and then started treatment (Fig. 1A). After 3 doses of Cisplatin, mice were euthanized, and flow cytometry revealed that the fraction of $ALDH^{high}CD44^{high}$ cells in UM-PDX-HACC-5

tumors was increased (P=0.018) in mice treated with Cisplatin (Fig. 1B,C). To evaluate the effect of platinum-based chemotherapeutic agents on ACC tumor cell density, UM-HACC cells were treated with increasing concentrations of Cisplatin or Carboplatin for 24 to 72 hours and SRB assays were performed. We observed that the half maximal inhibitory concentration (IC_{50}) for Cisplatin ranged between 3.4-26.2 μM and for Carboplatin from 22.9-46.8 μM for 72-hour treatment (Supplementary Fig. 1). *In vitro,* we observed a similar trend, *i.e.* Cisplatin (and Carboplatin) caused a dose-dependent increase in the fraction of $ALDH^{high}CD44^{high}$ cells in the three ACC cell lines tested (Fig. 1D,E).

To assess the effect of Cisplatin and Carboplatin on stemness and self-renewal potential, we performed western blots and salisphere assays. Both cytotoxic drugs induced expression of the major activator of stem cell self-renewal Bmi-1 and of Oct4, a key stem cell factor in embryogenesis and regulator of pluripotency of cancer stem cells [28] (Fig. 2A,B). Cisplatin and Carboplatin also increased the number of salispheres in a dose-dependent manner (Fig. 2C-E; Supplementary Fig. 2). Collectively, these experiments demonstrated that platinum-based drugs induce stemness features in ACC cells *in vitro*. As these results showed that Cisplatin and Carboplatin exhibit similar trends, we decided to focus the remaining studies on Cisplatin as our prototypic chemotherapeutic agent.

PTC596 inhibits ACC stemness *in vitro*

To examine the effect of PTC596 on ACC cell viability, we performed SRB assays. UM-ACC cells were treated with increasing concentrations of PTC596 with or without 1 μM Cisplatin. We observed that UM-ACC cells (particularly UM-HACC-2A) are particularly sensitive to PTC596 with IC_{50} in the low nanomolar range (Supplementary Fig. 3). Baseline Bmi-1 expression was stronger in UM-HACC-2A cells than in UM-HACC-14 or low passage primary UM-HACC-6 cells (Supplementary Fig. 3B), which might explain the unique sensitivity of UM-HACC-2A to PTC596. Combination of PTC596 with Cisplatin showed lower IC_{50} in UM-HACC-2A and UM-HACC-14 cells, when compared to PTC596 alone (Supplementary Fig. 3A).

To evaluate the effect of PTC596 on ACC stemness, we performed flow cytometry and observed that the fraction of $ALDH^{high}CD44^{high}$ cells decreased with increasing concentrations of PTC596 in all ACC cell lines (Fig. 3A). To investigate the effect of PTC596 and Cisplatin on CSC and non-CSC, ACC cells were sorted for $ALDH^{high}CD44^{high}$ and $ALDH^{low}CD44^{low}$ cells (Supplementary Fig. 3C). Western blots showed that the $ALDH^{high}CD44^{high}$ cells exhibited higher baseline Bmi-1 expression compared to $ALDH^{low}CD44^{low}$ cells (Fig. 3B). Then, we treated sorted cells with PTC596 or Cisplatin for a short period of time and stained them with *in situ* TUNEL to identify apoptotic cells. Surprisingly, Cisplatin caused more apoptosis in the non-CSCs ($ALDH^{low}CD44^{low}$) cells, whereas PTC596 caused more apoptosis of CSC ($ALDH^{high}CD44^{high}$) cells (Fig. 3C,D). Consistent with this finding, we observed that the expression of BAX (inducer of apoptosis) was increased in PTC596-treated $ALDH^{high}CD44^{high}$ cells (Supplementary Fig. 3D). These results indicate preferential induction of apoptosis of $ALDH^{high}CD44^{high}$ cells as a potential mechanism to explain the reduction of CSC fraction observed upon PTC596 treatment, which is consistent with other therapies that induce preferential apoptosis of CSCs [29]. To

understand the impact of PTC596 on a master regulator of stemness, we performed western blots that showed that inhibition Bmi-1 correlates with downregulation of Oct4 (Fig. 3E,F). Further, we observed a dose-dependent decrease in the number of salispheres upon treatment with low nanomolar concentrations of PTC596 (Fig. 3G).

PTC596 downregulates expression of pro-survival proteins in ACC cells

To determine pathways involved in PTC596-induced cell death, we treated UM-HACC-2A cells with Cisplatin, PTC596, or PTC596/Cisplatin together and used an apoptosis protein array. Combination therapy caused higher expression of pro-apoptotic proteins (*e.g.* BAX) when compared with single agent (Fig. 4A). Interestingly, Cisplatin or PTC596 alone showed reciprocal and inverse effects on the expression of several pro-survival proteins (*e.g.* Claspin) in ACC cells (Fig. 4A,B). To verify these results, we used western blots that showed that while Cisplatin induced Bmi-1, Claspin and Mcl-1 expression (Fig. 4C), PTC596 inhibited expression of these proteins. Indeed, we observed both dose- and time-dependent downregulation of Claspin and Mcl-1 in cells treated with PTC596 (Fig. 4D). Mcl-1 was included in these analyses as it has been shown that PTC596 downregulates expression of this pro-survival protein [30].

Claspin as a potential downstream effector of Bmi-1 in the regulation of ACC stemness

We observed that the modulation of Claspin expression upon treatment with Cisplatin or PTC596 followed a similar trend as Bmi-1 expression (Fig. 4C,D). Immunofluorescence staining of ACC PDX tumors showed co-expression of Claspin and Bmi-1 (Fig. 4E; Supplementary Fig. 4A). Notably, the number of cells co-expressing Bmi-1 and Claspin increased with Cisplatin treatment and decreased with PTC596 or combination therapy. Interestingly, the phosphorylation of Chk1, a known downstream effector of Claspin [31], was also downregulated upon PTC596 treatment (Fig. 4D). Considering that Chk1 sensitizes tumor cells and CSCs to chemotherapy [32,33], we explored the possibility that Bmi-1 signaling through Claspin could play a role in ACC stemness. To evaluate this possibility, we silenced Claspin in UM-HACC-2A and UM-HACC-14 cells (Fig. 4F). Western blotting demonstrated no feedback loop affecting Bmi-1 and Mcl-1 expression in Claspin-silenced ACC cells. To investigate whether silencing Claspin affects cell proliferation, SRB assays were performed and showed no difference in cell density between Claspin-silenced cells and vector control cells (Supplementary Fig. 4B). We also observed that the expression of Proliferating Cell Nuclear Antigen (PCNA) was unchanged when Claspin-silenced cells were compared to controls (Supplementary Fig. 4C). However, we observed a significant decrease in the fraction of CSCs ($ALDH^{high}$) cells upon Claspin silencing (Fig. 4G) which correlated with a decrease in salisphere-forming ability (Fig. 4H). Collectively, these data suggest that Claspin might serve as a downstream effector of Bmi-1 and play a role in the regulation of ACC stemness.

PTC596 blocks Cisplatin-induced ACC stemness

To examine the impact of combination therapy on ACC stemness, we treated UM-HACC cells with PTC596 and/or Cisplatin and then performed flow cytometry to assess ALDH activity and CD44 expression. As expected, single agent Cisplatin increased the fraction of ACC CSCs, while PTC596 decreased the CSC fraction (Fig. 5A, B). However, when

PTC596 and Cisplatin were combined, the CSC fraction was comparable to PTC596 alone and below vehicle-treated controls (UM-HACC-2A, UM-HACC-6). To further assess the effect of combination therapy on ACC stemness and self-renewal we performed primary and secondary salisphere assays, as serial passaging of salispheres provides an indication of impact of treatment on stem cell self-renewal. Combination therapy with Cisplatin and PTC596 caused a marked decrease in the number of primary and particularly secondary salispheres, when compared to vehicle control or Cisplatin alone (Fig. 5C,D; Supplementary Fig. 5A,B).

To explore the effect of combination therapy *in vivo*, we designed a short-term study using our ACC PDX model UM-PDX-HACC-5. When the average tumor volume reached 300 mm^3, mice were randomly allocated to 4 groups (n=10), as follows: vehicle, Cisplatin, PTC596, or Cisplatin + PTC596 (Fig. 6A). Drugs were administered on day 0 and 4, and mice were euthanized on day 5. We observed that Cisplatin alone increased the CSC fraction, while both PTC596 alone and combination therapy caused a decrease in the CSC fraction ($P<0.05$) when compared with vehicle or Cisplatin alone (Fig. 6B,C). Western blotting of PDX tumor lysates showed similar trends as Cisplatin alone induced Bmi-1 expression, while combination therapy caused downregulation of Bmi-1 and Claspin as compared to vehicle control (Fig. 6D,E). Of note, the graph in Fig. 6E depicts data from 5 tumors per experimental condition. To confirm that PTC596 was effective in inhibiting Bmi-1 *in vivo* even in presence of Cisplatin, we performed immunofluorescence staining and observed that very few cells were stained for Bmi-1 when PTC596 was used alone or in combination with Cisplatin (Fig. 6F,G).

Combination therapy of PTC596 and Cisplatin prevents tumor relapse

While the previous *in vivo* experiments were short-term studies focused on impacts of therapy on cancer stemness, here we performed preclinical studies designed to evaluate impacts on tumor growth and tumor relapse. When average tumor size reached 400 mm^3, mice were randomly allocated into 4 groups (n=8). In this study, 5 mg/kg Cisplatin was given once a week [26] and 5 mg/kg PTC596 was given twice a week. Single agent Cisplatin or PTC596 caused a modest slowdown in tumor growth (Fig. 7A,C). The limited response by Cisplatin treatment in this pre-clinical model was similar to what is observed in humans [34,35]. In contrast, combination PTC596 and Cisplatin prevented tumor growth (Fig. 7A). Importantly, mice exhibited <20% weight loss compared to pretreatment weight, which was the cutoff of our IACUC protocol (Fig. 7B). Kaplan-Meier curves using a 2-fold increase in tumor volume as compared with pretreatment size as criterion for "event" showed that PTC596/Cisplatin combination extended time to failure when compared with vehicle control ($P=0.0004$), single agent Cisplatin ($P=0.0246$) or single agent PTC596 ($P=0.0110$) (Fig. 7D). To better understand anti-tumor effects *in vivo*, we stained the tissue slides for TUNEL and observed more apoptotic cells in mice that received combination therapy when compared with vehicle ($P=0.013$) (Fig. 7E,F). And finally, to assess whether these therapies were effective in suppressing tumor relapse, we generated PDX ACC tumors and treated mice with either vehicle (n=7), weekly 5 mg/kg Cisplatin (n=7), or combination of weekly 5 mg/kg Cisplatin + twice a week 5 mg /kg PTC596 (n=6). Mice were treated for 2 weeks and then treatment was discontinued. Tumor relapse was assessed twice/week for 150 days.

Kaplan-Meier analysis showed that combination treatment significantly prevented tumor regrowth when compared to vehicle alone (P=0.042) or Cisplatin alone (P=0.034) (Fig. 7G).

Discussion

Resistance to systemic therapy is a major problem in management of patients with advanced salivary gland ACC. As such, treatment is typically limited to surgery and local radiation therapy. Considering the high incidence of late, albeit frequent tumor relapse experienced by these patients, the development of a safe and effective systemic therapy is urgently needed. Given that CSCs have been implicated in therapeutic resistance and cancer progression in many tumor types [36,37], we conducted a series of experiments to test the hypothesis that effective therapeutic ablation of CSCs prevent ACC tumor relapse.

Platinum-based drugs have been used in the treatment of ACC [15]. Emerging evidence demonstrates that these drugs can actually cause a shift towards self-renewal in tumorigenic CSC in certain tumors such as glioblastoma and HNSCC [16,17]. Knowing that Bmi-1 is an important epigenetic factor that regulates stem cell self-renewal, that Bmi-1 is involved in the recruitment of DNA repair factors and thereby enabling DNA damage [38], and that high Bmi-1 correlates with a low metastasis-free survival [23], we became interested in looking at the role of Bmi-1 in ACC stemness and response to treatment. PTC596 was then selected as our prototypic and clinically relevant small molecule inhibitor to evaluate the impact of a Bmi-1-targeted therapy on *in vitro* and preclinical models of ACC.

Here, we showed that Cisplatin or Carboplatin induce Bmi-1 expression and increase the ACC CSC fraction. We also reported that targeted inhibition of Bmi-1 signaling with PTC596 blocked Cisplatin-induced Bmi-1 expression and decreased the ACC CSC fraction. These results may represent a mechanism to explain the poor prognosis of patients with ACC who were treated with platinum-based agents, as CSCs are resistant to these agents may promote tumor relapse [36,37]. Considering that CSCs represent only a small proportion of cells within the tumor (<5%), using only a CSC-targeted approach does not result in tumor shrinkage. As such, one may have to consider a combination therapy that targets both CSC and bulk tumor cells to “de-bulk” the primary tumor while preventing CSC-mediated tumor relapse.

We have also observed that PTC596 treatment downregulated key pro-survival proteins such as Mcl-1 and Claspin. Mcl-1 is a Bcl-2 family protein that enhances cell survival [39] and is essential for drug resistance and expansion of CSCs in acute myeloid leukemia and breast cancers [40,41]. Bmi-1 was shown to upregulate Mcl-1 expression [30,42], possibly via the PI3K/Akt pathway [43], which is activated by Bmi-1 [44]. Claspin is another pro-survival protein that regulates DNA damage repair via the Claspin-ATR-Chk1 axis [31]. Bmi-1 and Claspin may have a correlation via beta-transduction repeat containing protein (βTrCP), a critical E3 ubiquitin ligase that regulates protein stability [45,46]. In addition, it has been postulated that Bmi-1 can be directly involved in the phosphorylation of Chk1, which is downstream of Claspin [47]. And finally, it has been shown that inhibiting Chk1 suppresses CSCs and improves the sensitivity to cytotoxic chemotherapy [32]. While we showed that targeted inhibition of Bmi-1 results in downstream downregulation of Claspin,

future research will evaluate the possibility of direct targeting of Claspin as an anti-CSC strategy.

We have first showed that cisplatin induces Bmi-1 expression and CSC self-renewal in HNSCC [17]. Here, we extended these observations to ACC and observed similar trends for both cisplatin and carboplatin. From these data, we concluded that with at least two platinum-based agents, the increase in Bmi-1 expression correlates with an increase in the CSC fraction. To better understand these results mechanistically, we performed experiments that showed that cisplatin is very effective at inducing apoptosis of non-CSCs while being ineffective at killing CSCs. In contrast, inhibition of Bmi-1 with PTC596 is effective at inducing apoptosis of CSCs while being ineffective at killing non-CSCs. We also observed that while cisplatin and carboplatin increase the number of salispheres, PTC596 decreases the number of salispheres. We concluded that while both drugs (platinum-based agents and PTC596) used as monotherapy cause a modest decrease in tumor volume, the target cell populations that are killed by each agent is different.

Conclusion

A key premise of anti-CSC therapies is that effective ablation of CSCs prevents tumor relapse and tumor dissemination [37]. Here, we tested this premise by administering Cisplatin alone or Cisplatin combined with PTC596 for 2 weeks, then stopping treatment and following up for tumor regrowth in the mice. While all tumors treated with Cisplatin only or vehicle relapsed within 30 days, approximately 30% of the tumors treated with Cisplatin + PTC596 did not relapse for a period of 150 days. These data suggest that adding PTC596 to the cytotoxic agent decreases the tumorigenic potential of residual ACC tumor cells, possibly by eliminating the CSCs (as we showed in several short-term experiments presented here). These exciting results provide preclinical evidence for a new treatment strategy based on targeted ablation of CSCs with a small molecule inhibitor of Bmi-1 in combination with a platinum-based cytotoxic therapy for treatment of patients with salivary gland adenoid cystic carcinoma.

Supplementary Material

Refer to Web version on PubMed Central for supplementary material.

Acknowledgments:

We thank the patients for kindly donating the tumor specimens used to generate the cell lines and xenograft models of adenoid cystic carcinoma that enabled this research project. We also thank the University of Michigan Histology and Flow Cytometry Cores for their skillful support. We also thank Takafumi Nakano for his excellent technical support.

Funding:

This work was funded by the National Institutes of Health [grant numbers F30-DE029097, R01-DE021139 and R01-DE023220] and by the Society for Promotion of International Oto-Rhino-Laryngology.

References

[1]. Spiro RH, Huvos AG, Strong EW. Adenoid cystic carcinoma of salivary origin: A clinicopathologic study of 242 cases. Am J Surg 1974;128:512–20. https://doi.org/10.1016/0002-9610(74)90265-7. [PubMed: 4371368]

[2]. Dodd RL, Slevin NJ. Salivary gland adenoid cystic carcinoma: A review of chemotherapy and molecular therapies. Oral Oncol 2006;42:759–69. 10.1016/j.oraloncology.2006.01.001. [PubMed: 16757203]

[3]. Khan AJ, Digiovanna MP, Ross DA, Sasaki CT, Carter D, Son YH, et al. Adenoid cystic carcinoma: A retrospective clinical review. Int J Cancer 2001;96:149–58. 10.1002/ijc.1013. [PubMed: 11410883]

[4]. Lim WS, Oh JS, Roh JL, Kim JS, Kim SJ, Choi SH, et al. Prediction of distant metastasis and survival in adenoid cystic carcinoma using quantitative 18F-FDG PET/CT measurements. Oral Oncol 2018;77:98–104. 10.1016/j.oraloncology.2017.12.013. [PubMed: 29362133]

[5]. Ferrarotto R, Mitani Y, Diao L, Guijarro I, Wang J, Zweidler-McKay P, et al. Activating NOTCH1 mutations define a distinct subgroup of patients with adenoid cystic carcinoma who have poor prognosis, propensity to bone and liver metastasis, and potential responsiveness to Notch1 inhibitors. J Clin Oncol 2017;35:352–60. 10.1200/JCO.2016.67.5264. [PubMed: 27870570]

[6]. Rodriguez-Russo CA, Junn JC, Yom SS, Bakst RL. Radiation Therapy for Adenoid Cystic Carcinoma of the Head and Neck. Cancers (Basel) 2021;13:6335. 10.3390/cancers13246335. [PubMed: 34944955]

[7]. Chummun S, McLean NR, Kelly CG, Dawes PJDK, Fellows S, Meikle D, et al. Adenoid cystic carcinoma of the head and neck. Br J Plast Surg 2001;54:476–80. 10.1054/bjps.2001.3636. [PubMed: 11513507]

[8]. Chen AM, Bucci MK, Weinberg V, Garcia J, Quivey JM, Schechter NR, et al. Adenoid cystic carcinoma of the head and neck treated by surgery with or without postoperative radiation therapy: Prognostic features of recurrence. Int J Radiat Oncol Biol Phys 2006;66:152–9. 10.1016/j.ijrobp.2006.04.014. [PubMed: 16904520]

[9]. Garden AS, Weber RS, Morrison WH, Ang KK, Peters LJ. The influence of positive margins and nerve invasion in adenoid cystic carcinoma of the head and neck treated with surgery and radiation. Int J Radiat Oncol 1995;32:619–26. https://doi.org/10.1016/0360-3016(95)00122-F.

[10]. Adams A, Warner K, Nör JE. Salivary gland cancer stem cells. Oral Oncol 2013;49:845–53. 10.1016/j.oraloncology.2013.05.013. [PubMed: 23810400]

[11]. Lawson DA, Bhakta NR, Kessenbrock K, Prummel KD, Yu Y, Takai K, et al. Single-cell analysis reveals a stem-cell program in human metastatic breast cancer cells. Nature 2015;526:131–5. 10.1038/nature15260. [PubMed: 26416748]

[12]. Cojoc M, Mäbert K, Muders MH, Dubrovska A. A role for cancer stem cells in therapy resistance: Cellular and molecular mechanisms. Semin Cancer Biol 2015;31:16–27. 10.1016/j.semcancer.2014.06.004. [PubMed: 24956577]

[13]. Sun S, Wang Z. ALDHhigh adenoid cystic carcinoma cells display cancer stem cell properties and are responsible for mediating metastasis. Biochem Biophys Res Commun 2010;396:843–8. 10.1016/j.bbrc.2010.04.170. [PubMed: 20450887]

[14]. Keysar SB, Eagles JR, Miller B, Jackson BC, Chowdhury FN, Reisinger J, et al. Salivary Gland Cancer Patient-Derived Xenografts Enable Characterization of Cancer Stem Cells and New Gene Events Associated with Tumor Progression. Clin Cancer Res 2018;24:2935–43. 10.1158/1078-0432.CCR-17-3871. [PubMed: 29555661]

[15]. Sahara S, Herzog AE, Nör JE. Systemic therapies for salivary gland adenoid cystic carcinoma. Am J Cancer Res 2021;11:4092–110. [PubMed: 34659878]

[16]. Chen J, Li Y, Yu T-S, McKay RM, Burns DK, Kernie SG, et al. A restricted cell population propagates glioblastoma growth after chemotherapy. Nature 2012;488:522–6. 10.1038/nature11287. [PubMed: 22854781]

[17]. Nör C, Zhang Z, Warner KA, Bernardi L, Visioli F, Helman JI, et al. Cisplatin Induces Bmi-1 and Enhances the Stem Cell Fraction in Head and Neck Cancer. Neoplasia 2014;16:137–W8. 10.1593/neo.131744. [PubMed: 24709421]

[18]. Almeida LO, Guimarães DM, Martins MD, Martins MAT, Warner KA, Nör JE, et al. Unlocking the chromatin of adenoid cystic carcinomas using HDAC inhibitors sensitize cancer stem cells to cisplatin and induces tumor senescence. Stem Cell Res 2017;21:94–105. 10.1016/j.scr.2017.04.003. [PubMed: 28426972]

[19]. Nakano T, Warner KA, Oklejas AE, Zhang Z, Rodriguez-Ramirez C, Shuman AG, et al. mTOR Inhibition Ablates Cisplatin-Resistant Salivary Gland Cancer Stem Cells. J Dent Res 2021;100:377–86. 10.1177/0022034520965141. [PubMed: 33073679]

[20]. Herzog AE, Warner KA, Zhang Z, Bellile E, Bhagat MA, Castilho RM, et al. The IL-6R and Bmi-1 axis controls self-renewal and chemoresistance of head and neck cancer stem cells. Cell Death Dis 2021;12:988. 10.1038/s41419-021-04268-5. [PubMed: 34689150]

[21]. Chen D, Wu M, Li Y, Chang I, Yuan Q, Ekimyan-Salvo M, et al. Targeting BMI1 + Cancer Stem Cells Overcomes Chemoresistance and Inhibits Metastases in Squamous Cell Carcinoma. Cell Stem Cell 2017;20:621–634.e6. 10.1016/j.stem.2017.02.003. [PubMed: 28285905]

[22]. Jia L, Zhang W, Wang C-Y. BMI1 Inhibition Eliminates Residual Cancer Stem Cells after PD1 Blockade and Activates Antitumor Immunity to Prevent Metastasis and Relapse. Cell Stem Cell 2020;27:238–253.e6. 10.1016/j.stem.2020.06.022. [PubMed: 32697949]

[23]. Yi C, Li B, Zhou C-X. Bmi-1 expression predicts prognosis in salivary adenoid cystic carcinoma and correlates with epithelial-mesenchymal transition–related factors. Ann Diagn Pathol 2016;22:38–44. https://doi.org/10.1016/j.anndiagpath.2015.10.015. [PubMed: 27180058]

[24]. Shapiro GI, O'Mara E, Laskin OL, Gao L, Baird JD, Spiegel RJ, et al. Pharmacokinetics and Safety of PTC596, a Novel Tubulin-Binding Agent, in Subjects With Advanced Solid Tumors. Clin Pharmacol Drug Dev 2021;10:940–9. 10.1002/cpdd.904. [PubMed: 33440067]

[25]. Warner KA, Oklejas AE, Pearson AT, Zhang Z, Wu W, Divi V, et al. UM-HACC-2A: MYB-NFIB fusion-positive human adenoid cystic carcinoma cell line. Oral Oncol 2018;87:21–8. 10.1016/j.oraloncology.2018.10.012. [PubMed: 30527239]

[26]. Pearson AT, Herwig KA, Warner KA, Nör F, Tice D, Martins MD, Jackson TL, Nör JE. Patient Derived Xenograft (PDX) Tumors Increase Growth Rate with Time. Oncotarget 2016;7(7):7993–8005. https://www.oncotarget.com/article/6919/text/ [PubMed: 26783960]

[27]. Nör F, Warner KA, Zhang Z, Acasigua GA, Pearson AT, Kerk SA, et al. Therapeutic Inhibition of the MDM2–p53 Interaction Prevents Recurrence of Adenoid Cystic Carcinomas. Clin Cancer Res 2017;23:1036–48. 10.1158/1078-0432.CCR-16-1235. [PubMed: 27550999]

[28]. Mohiuddin IS, Wei S-J, Kang MH. Role of OCT4 in cancer stem-like cells and chemotherapy resistance. Biochim Biophys Acta - Mol Basis Dis 2020;1866:165432. 10.1016/j.bbadis.2019.03.005. [PubMed: 30904611]

[29]. Andrade NP, Warner KA, Zhang Z, Pearson AT, Mantesso A, Guimaraēs DM, et al. Survival of salivary gland cancer stem cells requires mTOR signaling. Cell Death Dis 2021;12:108. 10.1038/s41419-021-03391-7. [PubMed: 33479203]

[30]. Nishida Y, Maeda A, Kim MJ, Cao L, Kubota Y, Ishizawa J, et al. The novel BMI-1 inhibitor PTC596 downregulates MCL-1 and induces p53-independent mitochondrial apoptosis in acute myeloid leukemia progenitor cells. Blood Cancer J 2017;7:1–9. 10.1038/bcj.2017.8.

[31]. Azenha D, Lopes MC, Martins TC. Claspin functions in cell homeostasis—A link to cancer? DNA Repair (Amst) 2017;59:27–33. 10.1016/j.dnarep.2017.09.002. [PubMed: 28942358]

[32]. Venkatesha VA, Parsels LA, Parsels JD, Zhao L, Zabludoff SD, Simeone DM, et al. Sensitization of pancreatic cancer stem cells to gemcitabine by Chk1 inhibition. Neoplasia (United States) 2012;14:519–25. 10.1593/neo.12538.

[33]. Saini P, Li Y, Dobbelstein M. Wee1 is required to sustain ATR/Chk1 signaling upon replicative stress. Oncotarget 2015;6:13072–87. 10.18632/oncotarget.3865. [PubMed: 25965828]

[34]. Ghosal N, Mais K, Shenjere P, Julyan P, Hastings D, Ward T, et al. Phase II study of cisplatin and imatinib in advanced salivary adenoid cystic carcinoma. Br J Oral Maxillofac Surg 2011;49:510–5. 10.1016/j.bjoms.2010.09.013. [PubMed: 21071117]

[35]. Licitra L, Marchini S, Spinazzè S, Rossi A, Rocca A, Grandi C, et al. Cisplatin in advanced salivary gland carcinoma. A phase II study of 25 patients. Cancer 1991;68:1874–7. 10.1002/1097-0142(19911101)68:9<1874::AID-CNCR2820680904>3.0.CO;2-S. [PubMed: 1913539]

[36]. Korkaya H, Kim G, Davis A, Malik F, Henry NL, Ithimakin S, et al. Activation of an IL6 Inflammatory Loop Mediates Trastuzumab Resistance in HER2+ Breast Cancer by Expanding the Cancer Stem Cell Population. Mol Cell 2012;47:570–84. 10.1016/j.molcel.2012.06.014. [PubMed: 22819326]

[37]. Chinn SB, Darr OA, Owen JH, Bellile E, McHugh JB, Spector ME, et al. Cancer stem cells: Mediators of tumorigenesis and metastasis in head and neck squamous cell carcinoma. Head Neck 2015;37:317–26. 10.1002/hed.23600. [PubMed: 24415402]

[38]. Ismail IH, Andrin C, McDonald D, Hendzel MJ. BMI1-mediated histone ubiquitylation promotes DNA double-strand break repair. J Cell Biol 2010;191:45–60. 10.1083/jcb.201003034. [PubMed: 20921134]

[39]. Yarbrough WG, Panaccione A, Chang MT, Ivanov SV. Clinical and molecular insights into adenoid cystic carcinoma: Neural crest-like stemness as a target. Laryngoscope Investig Otolaryngol 2016;1:60–77. 10.1002/lio2.22.

[40]. Hermanson DL, Das SG, Li Y, Xing C. Overexpression of Mcl-1 Confers Multidrug Resistance, Whereas Topoisomerase II β Downregulation Introduces Mitoxantrone-Specific Drug Resistance in Acute Myeloid Leukemia. Mol Pharmacol 2013;84:236–43. 10.1124/mol.113.086140. [PubMed: 23696245]

[41]. Lee K, Giltnane JM, Balko JM, Schwarz LJ, Guerrero-Zotano AL, Hutchinson KE, et al. MYC and MCL1 Cooperatively Promote Chemotherapy-Resistant Breast Cancer Stem Cells via Regulation of Mitochondrial Oxidative Phosphorylation. Cell Metab 2017;26:633–647.e7. 10.1016/j.cmet.2017.09.009. [PubMed: 28978427]

[42]. Gao R, Chen S, Kobayashi M, Yu H, Zhang Y, Wan Y, et al. Bmi1 Promotes Erythroid Development Through Regulating Ribosome Biogenesis. Stem Cells 2015;33:925–38. 10.1002/stem.1896. [PubMed: 25385494]

[43]. Warr MR, Shore GC. Unique biology of Mcl-1: therapeutic opportunities in cancer. Curr Mol Med 2008;8:138–47. 10.2174/156652408783769580. [PubMed: 18336294]

[44]. Du R, Xia L, Ning X, Liu L, Sun W, Huang C, et al. Hypoxia-induced Bmi1 promotes renal tubular epithelial cell-mesenchymal transition and renal fibrosis via PI3K/Akt signal. Mol Biol Cell 2014;25:2650–9. 10.1091/mbc.E14-01-0044. [PubMed: 25009285]

[45]. Sahasrabuddhe AA, Dimri M, Bommi PV., Dimri GP. βTrCP regulates BMI1 protein turnover via ubiquitination and degradation. Cell Cycle 2011;10:1322–30. 10.4161/cc.10.8.15372. [PubMed: 21430439]

[46]. Smits VAJ, Cabrera E, Freire R, Gillespie DA. Claspin – checkpoint adaptor and DNA replication factor. FEBS J 2019;286:441–55. 10.1111/febs.14594. [PubMed: 29931808]

[47]. Fitieh A, Locke AJ, Mashayekhi F, Khaliqdina F, Sharma AK, Ismail IH. BMI-1 regulates DNA end resection and homologous recombination repair. Cell Rep 2022;38:110536. 10.1016/j.celrep.2022.110536. [PubMed: 35320715]

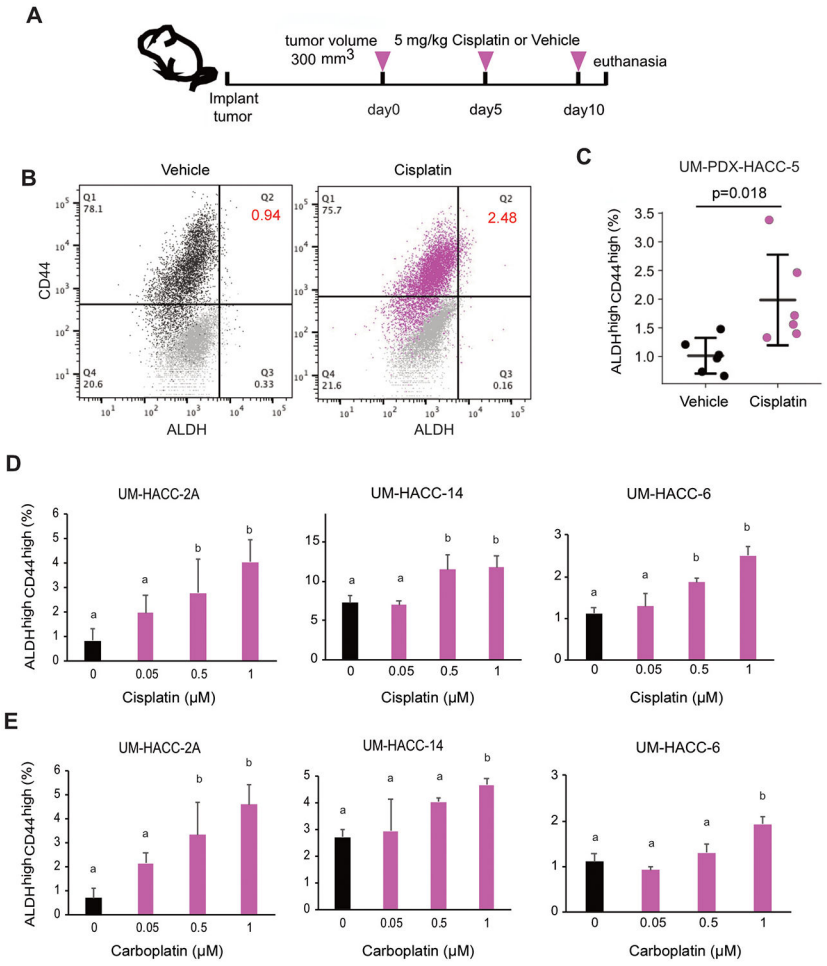

Fig. 1. Platinum-based drugs enhance ACC stemness.

A, Diagram depicting the treatment schema. Mice harboring UM-PDX-HACC-5 tumors were treated with either vehicle (Saline solution, *i.p.*, on days 0, 5, and 10) (n=6), or 5 mg/kg Cisplatin (*i.p.*, day 0, 5, and 10) (n=6). **B,** Representative flow cytometry dot plots depicting Aldefluor (ALDH activity), CD44 expression, and DEAB/IgG controls used for gating (gray). **C,** Graph depicting the fraction of CSCs, *i.e.* $ALDH^{high}CD44^{high}$ cells in UM-PDX-HACC-5 tumors treated with saline (vehicle) or 5 mg/kg Cisplatin. Statistical significance was determined by Student t-test. **D, E,** Bar graphs depicting the percentage of $ALDH^{high}CD44^{high}$ cells (UM-HACC-2A, UM-HACC-14, UM-HACC-6) in response to a 24-hour treatment with increasing concentrations (0 to 1 μM) of Cisplatin or Carboplatin. Values are presented as mean ± s.d. Different lowercase letters represent statistical significance at $P<0.05$ as determined by one-way ANOVA followed by post hoc tests.

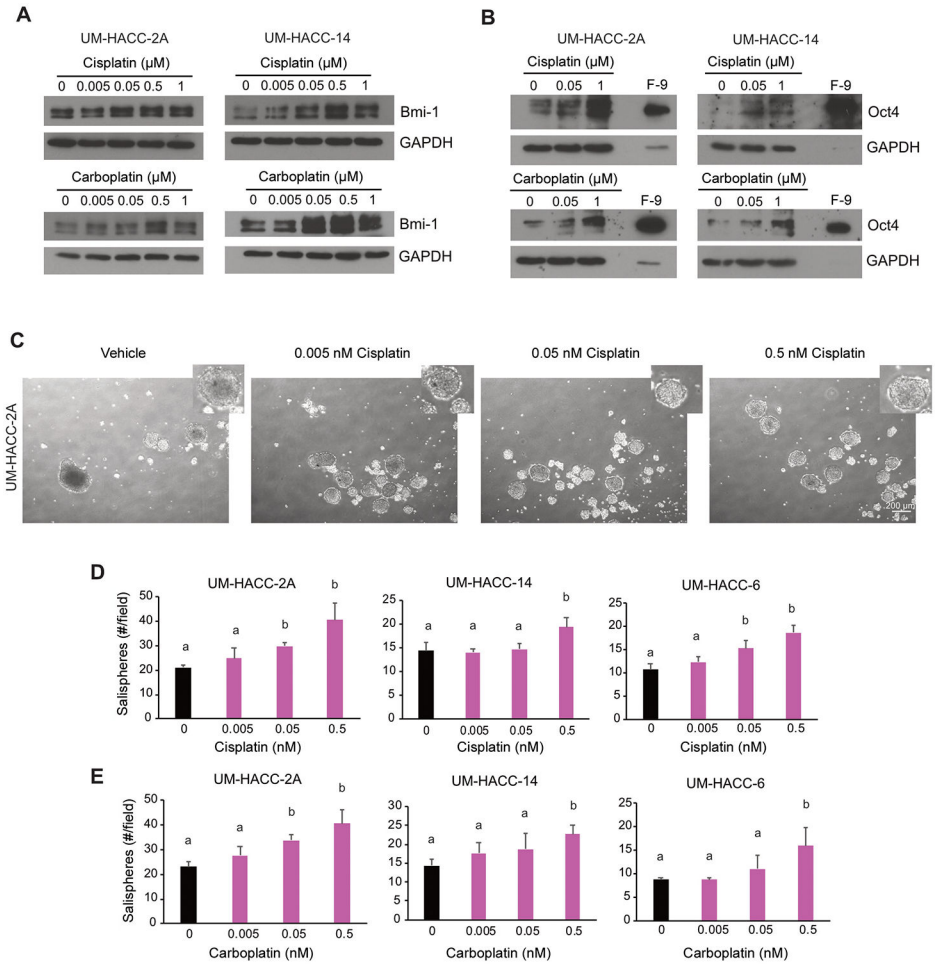

Fig. 2. Platinum-based drugs enhance ACC self-renewal.

A, B, Western blot analysis of UM-HACC-2A and UM-HACC-14 cells treated with 0-1 μM Cisplatin or Carboplatin for 24 hours. F-9 cell lysate was used as positive control for Oct4. **C,** Representative photographs of salispheres generated by UM-HACC-2A cells cultured in ultra-low attachment plates for 8 days and treated with 0 to 0.5 nM Cisplatin. Scale bars represent 200 μm. **D, E,** Bar graphs depicting the average number of salispheres per well (± s.d.) generated by UM-HACC-2A, UM-HACC-14, or UM-HACC- 6 cells treated with 0 to 0.5 nM Cisplatin or Carboplatin for 8 days. Different lowercase letters represent statistical significance at $P<0.05$ as determined by one-way ANOVA followed by post hoc tests.

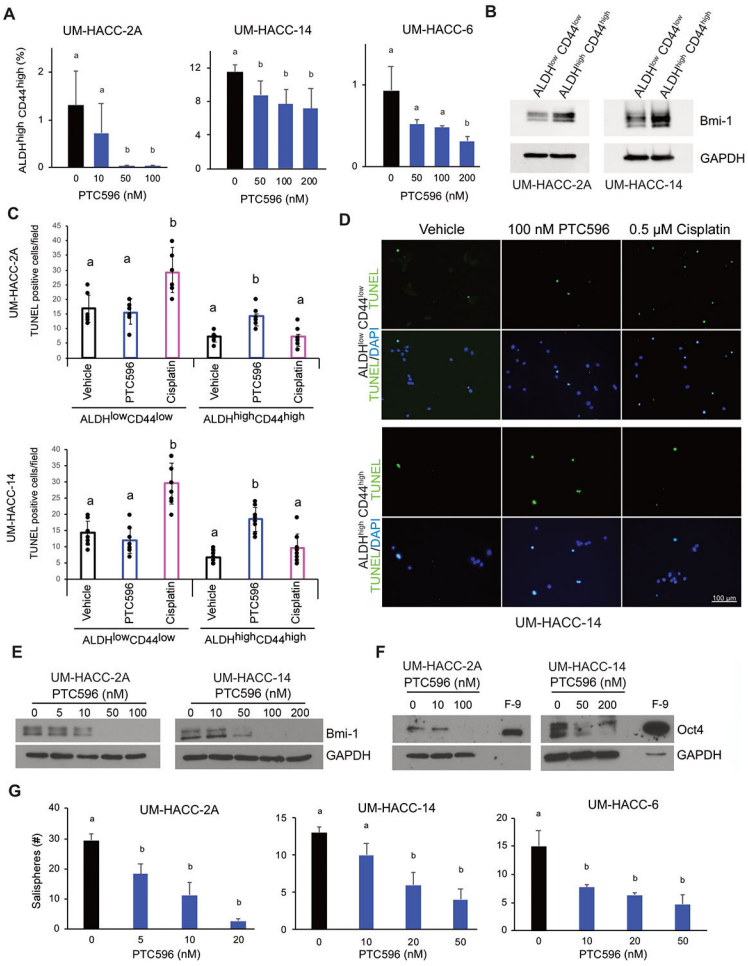

Fig. 3. Effect of Bmi-1 inhibition with PTC596 on cancer stem cells *in vitro*.

A, Bar graphs illustrate the percentage of ALDH^{high}CD44^{high} UM-HACC-2A, UM-HACC-14, or UM-HACC-6 cells treated with serial dilutions of PTC596 for 24 hours. **B,** Western blots to evaluate Bmi-1 expression on UM-HACC-2A and UM-HACC-14 cells sorted for ALDH and CD44. **C,** Graphs depicting the number of TUNEL-positive cells when UM-HACC-2A or UM-HACC-14 cells were sorted for ALDH/CD44, plated in chamber slides and treated with 0.5 μM Cisplatin or 100 nM PTC596. **D,** Representative images of UM-HACC-14 stained for TUNEL (apoptotic cells, green) and DAPI (nuclear staining, blue). **E, F,** Western blot analysis of UM-HACC-2A or UM-HACC-14 cells treated with PTC596 for 24 hours. F-9 cell lysate was used as positive control for Oct4. **G,** Bar graphs depicting the number of salispheres per well generated from UM-HACC-2A, UM-HACC-14, or UM-HACC-6 cells treated with increasing concentrations of PTC596. Values are presented as mean ± s.d. Different lowercase letters represent statistical significance at $P<0.05$ as determined by one-way ANOVA followed by post hoc tests.

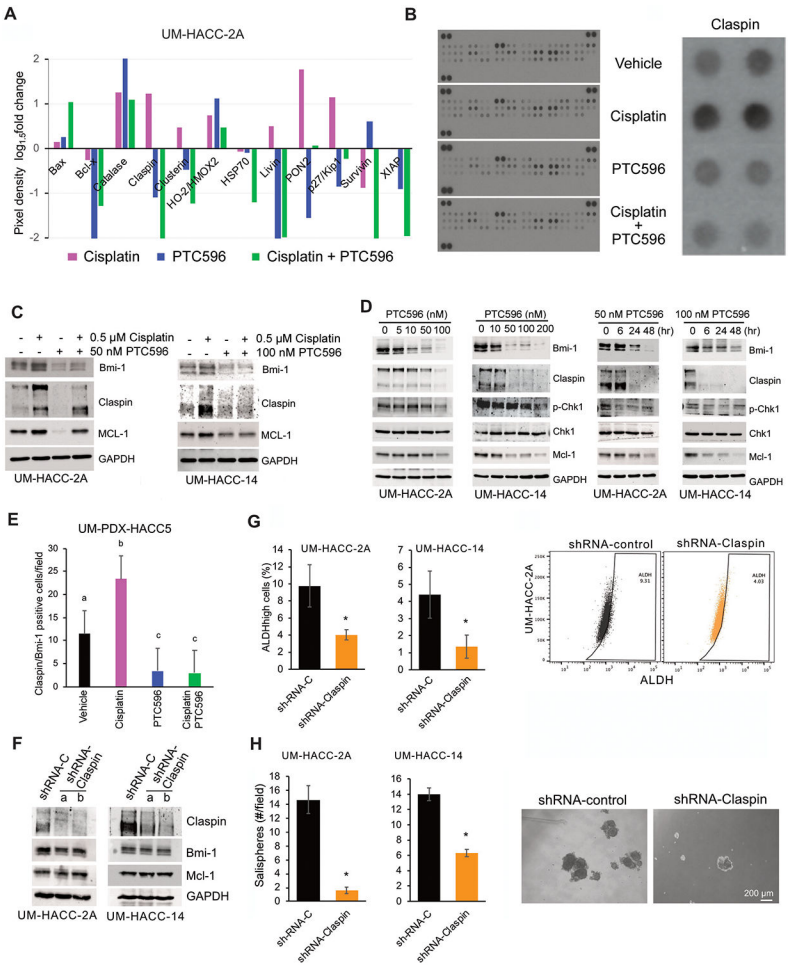

Fig. 4. Effect of PTC596 on the expression of pro-survival proteins Claspin and Mcl-1.

A, Graph depicting the fold change in protein density when compared to vehicle controls. Apoptosis protein array of UM-HACC-2A cells treated with vehicle, 0.5 μM Cisplatin, 50 nM PTC596, or 0.5 μM Cisplatin + 50 nM PTC596. **B,** Full scan of the protein array membranes and close-up images of the membrane depicting modulation in Claspin expression upon treatment. **C,** Western blot analysis of Claspin, Mcl-1, and Bmi-1 in UM-HACC-2A and UM-HACC-14 cells treated with vehicle, 0.5 μM Cisplatin, 50 nM PTC596, or 0.5 μM Cisplatin + 50 nM PTC596 for 24 hours. **D,** Western blot analysis of Bmi-1, Claspin, Chk1, and Mcl-1 in UM-HACC-2A and UM-HACC-14 cells treated with PTC596 in a dose-dependency (left) and in a time course (right) experiment. **E,** Bar graph illustrating the number of Claspin/Bmi-1-positive cells per high power field (HPF: 400X magnification) in UM- PDX-HACC-5 tissues retrieved from mice treated with 5 mg/kg Cisplatin and/or 5 mg/kg PTC596. Different lowercase letters represent statistical significance at $P<0.05$ as determined by one-way ANOVA followed by post hoc tests (Tukey's test). **F,** Western blot analysis of Claspin, Bmi-1, and Mcl-1 in UM-HACC-2A and UM-HACC-14 cells transduced with shRNA-control or shRNA-Claspin. **G,** Graph dot plot depicting flow cytometry analysis of ALDH activity in UM-HACC-2A and UM-HACC-14 cells transduced with shRNA-control or shRNA-Claspin. **H,** Bar graphs and representative

photographs of salispheres generated by UM-HACC-2A or UM-HACC-14 cells transduced with shRNA-control or shRNA-Claspin after 8 days in suspension culture. Asterisk indicates $P < 0.05$ as determined by Student t-test.

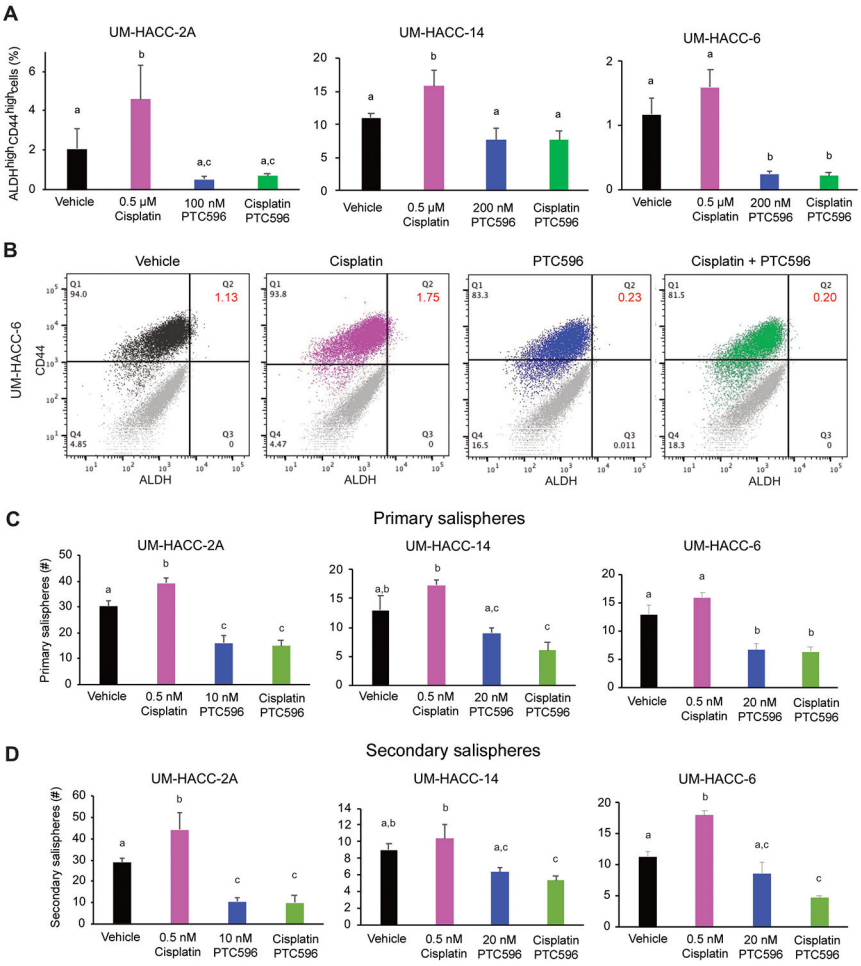

Fig. 5. Effect of combination PTC596 and Cisplatin on ACC cancer stem cells *in vitro*.

A, Bar graphs illustrate the percentage of $ALDH^{high}CD44^{high}$ in UM-HACC-2A, UM-HACC-14,and UM-HACC-6 cells treated with Cisplatin and/or PTC596. **B,** Representative flow cytometry dot plots depicting Aldefluor (ALDH activity) and CD44, as well as DEAB/IgG controls used for gating purposes. **C, D,** Bar graphs depicting the number of primary salispheres (C) and secondary salispheres (D) generated by UM-HACC-2A, UM-HACC-14, or UM-HACC-6 cells treated with Cisplatin and/or PTC596. Values are presented as mean ± s.d. Different lowercase letters represent statistical significance at $P<0.05$ as determined by one-way ANOVA followed by post hoc tests (Tukey's test).

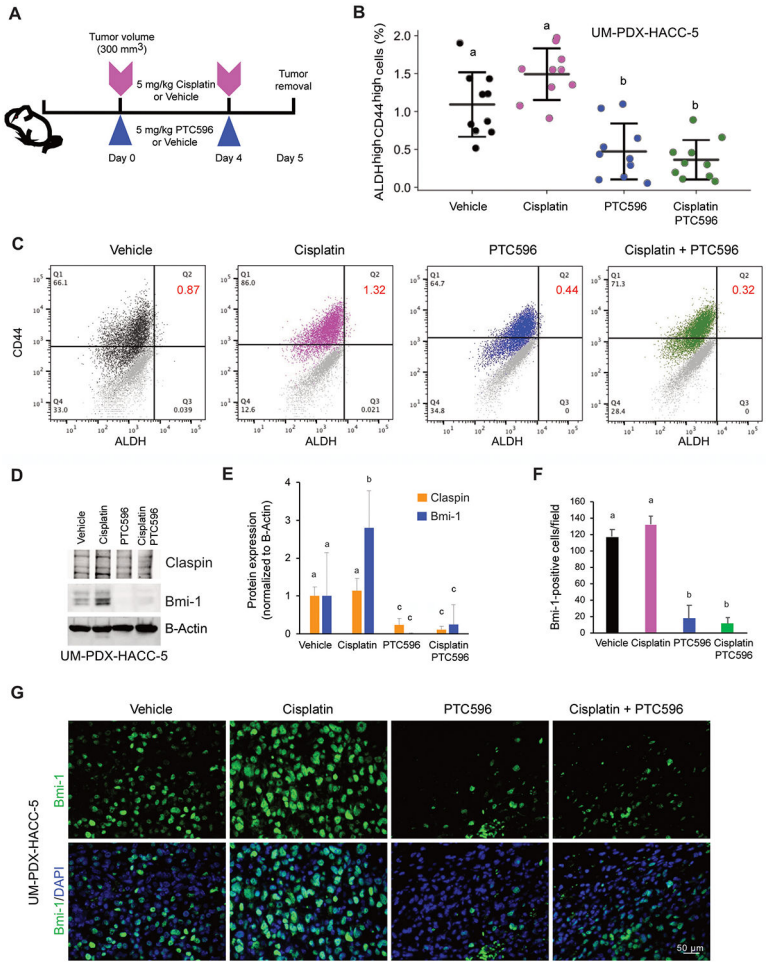

Fig. 6. Effect of combination PTC596 and Cisplatin on cancer stem cells *in vivo*.

A, Diagram depicting the treatment schema. Mice harboring UM-PDX-HACC-5 tumors were treated with vehicle, 5 mg/kg Cisplatin, 5 mg/kg PTC596, or combination 5 mg/kg Cisplatin + 5 mg/kg PTC596 for 5 days. **B,** Single cell suspensions were prepared from UM-PDX-HACC-5 tissues, stained for ALDH and CD44, and analyzed by flow cytometry. The graph illustrates the percentage of $ALDH^{high}CD44^{high}$ cells in UM-PDX-HACC-5 according to treatment. **C** Representative flow cytometry dot plots depicting Aldefluor (ALDH activity) and CD44, as well as DEAB/IgG controls used for gating purposes. **D, E,** Western blot of representative UM-PDX-HACC-5 tumor tissue lysates from each treatment group (D). Bar graph illustrates the quantification of Claspin and Bmi-1 normalized against Beta-actin (E). Band densities were quantified with ImageJ software (National Institutes of Health). **F,** Bar graph illustrating the number of Bmi-1-positive cells per high power field (400X magnification) in tumor tissues retrieved from UM-PDX-HACC −5 mice treated with 5 mg/kg Cisplatin, 5 mg/kg PTC596, or combination 5 mg/kg Cisplatin + 5 mg/kg PTC596 for 5 days. Values are presented as mean ± s.d. **G,** Representative images of UM-PDX-HACC-5 tumor tissue sections stained for Bmi-1 (green) and DAPI (blue). Scale bars represent 50 μm. Different lowercase letters represent statistical significance at $P<0.05$ as determined by one-way ANOVA followed by post hoc tests (Tukey's test).

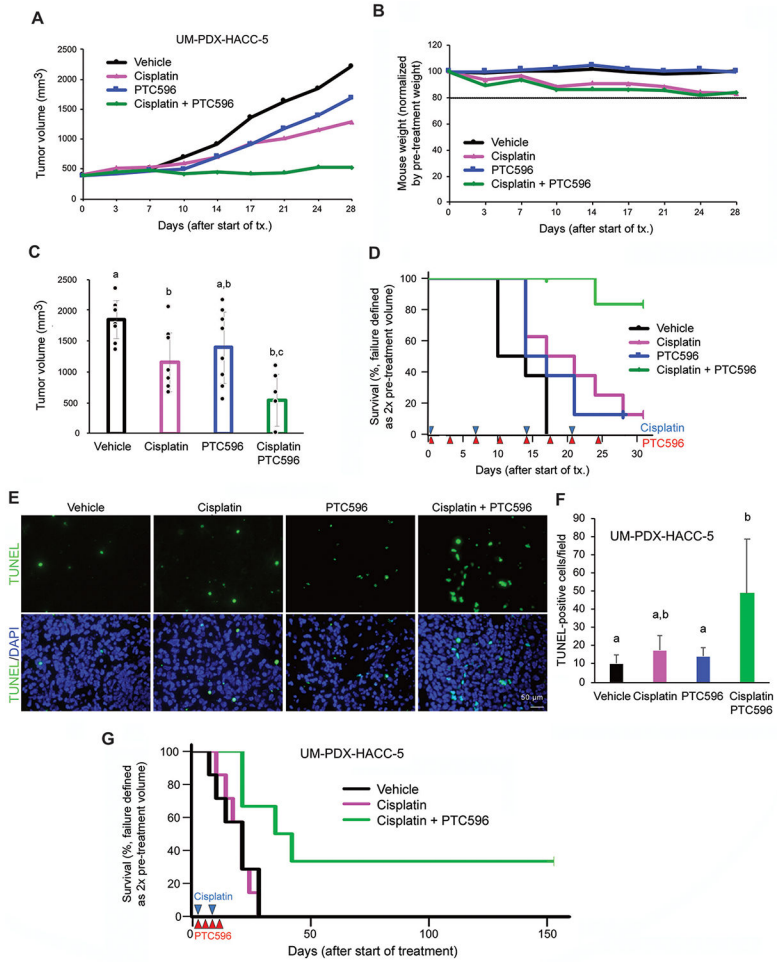

Fig. 7. Effect of combination therapy with PTC596 on long term efficacy.

A, UM-PDX-HACC-5 were tumors generated in immunodeficient mice. When an average tumor volume reached 400 mm^3, mice were randomly allocated to receive vehicle, 5 mg/kg Cisplatin, 5 mg/kg PTC596, or 5 mg/kg Cisplatin + 5 mg/kg PTC596 (n = 8 per group) for 24 days. Graph depicting tumor volume according to treatment. **B,** Graph depicting mouse weight during the experimental period. Data were normalized to pretreatment weight. Line indicates our cut-off weight loss of 20% for this experiment. **C,** Graph depicting tumor volume at the end of the experimental period. Different lowercase letters in graphs represent statistical significance at $P<0.05$ (**C,F**). **D,** Kaplan-Meier analysis was performed using a 2-fold increase in the tumor volume (as compared to pre-treatment volume) as a criterion for failure. **E,** Representative images of UM-PDX-HACC-5 tumor tissue sections stained for TUNEL (apoptotic cells, green) and DAPI (nuclei, blue). Scale bars represent 50 μm. **F,** Bar graph illustrating the number of TUNEL-positive cells per high power field (400X magnification) in tissues retrieved from UM-PDX-HACC-5. **G,** UM-PDX-HACC-5 tumors were generated in additional SCID mice. When an average tumor size reached 300 mm^3, mice were randomly allocated to the following treatment conditions: Vehicle (n=7), weekly 5 mg/kg Cisplatin (n =7) or combination of weekly 5 mg/kg Cisplatin + twice a week 5 mg/kg PTC596 (n=6). Mice were treated for only 2 weeks, then treatment stopped, and

tumors were measured weekly thereafter. Kaplan–Meier analysis was performed using as a criterion for failure a 2-fold increase in tumor volume as compared with pretreatment volume.